Contents lists available at ScienceDirect

Applied Energy

journal homepage: www.elsevier.com/locate/apenergy





Distributed model predictive control for joint coordination of demand response and optimal power flow with renewables in smart grid*

Ye Shi ^{a,*}, Hoang Duong Tuan ^b, Andrey V. Savkin ^c, Chin-Teng Lin ^d, Jian Guo Zhu ^e, H. Vincent Poor ^f

- ^a School of Information Science and Technology, Shanghaitech University, Shanghai, 201210, China
- b School of Electrical and Data Engineering, University of Technology, Sydney, NSW 2007, Australia
- ^c School of Electrical Engineering and Telecommunications, the University of New South Wales, NSW 2052, Australia
- d Australia Artificial Intelligence Institute, School of Computer Science, University of Technology, Sydney, NSW 2007, Australia
- ^e School of Electrical and Information Engineering, The University of Sydney, Sydney, NSW 2006, Australia
- f Department of Electrical Engineering, Princeton University, Princeton, NJ 08544, USA

ARTICLE INFO

Keywords: Smart grid Demand response Renewable energy resources Optimal power flow Distributed model predictive control Nonconvex optimization

ABSTRACT

Demand response is an emerging application of smart grid in exploiting timely interactions between utilities and their customers to improve the reliability and sustainability of power networks. This paper investigates the joint coordination of demand response and AC optimal power flow with curtailment of renewable energy resources to not only save the total amount of power generation costs, renewable energy curtailment costs and price-elastic demand costs but also manage the fluctuation of the overall power load under various types of demand response constraints and grid operational constraints. Its online implementation is very challenging since the future power demand is unpredictable with unknown statistics. Centralized and distributed model predictive control (CMPC and DMPC)-based methods are respectively proposed for the centralized and distributed computation of the online scheduling problem. The CMPC can provide a baseline solution for the DMPC. The DMPC is quite challenging that invokes distributed computation of a nonconvex optimization problem at each time slot. A novel alternating direction method of multipliers (ADMM)-based DMPC algorithm is proposed for this challenging DMPC. It involves an iterative subroutine computation during the update procedure of primal variables that can efficiently handle the difficult nonconvex constraints. Comprehensive experiments have been conducted to test the proposed methods. Simulation results show that the gap in objective values between the DMPC and its baseline counterpart (CMPC) are all within 1%, further verifying the effectiveness of the proposed ADMM-based DMPC algorithm.

1. Introduction

Smart grid is termed as the next-generation energy networks, which integrate distributed generators (DGs), renewable energy resources (RES), controllable loads, smart sensors and advanced metering infrastructure to enable two-way digital communications between utilities and their customers [1,2]. It is expected to provide sufficient and significant technology support for demand response (DR), in which the customers adapt their patterns of energy consumption in response to the fluctuation of electricity price or incentives provided by the utilities [3]. DR is widely accepted as a viable solution to promote

interactions between the utilities and customers in reducing the overall power load at peak hours or during system contingency for the system reliability and sustainability improvement [4]. Furthermore, by integrating DR, the overall plant cost and capital investment can be reduced and the upgrade of power networks can be flexibly postponed in the long term [5]. For example, integrating DR and energy storage in combined cooling, heating, and power systems can reduce system total cost by 14.66% [6]. Nowadays, DR is an indispensable component of the smart grid so it is certainly an attractive research topic.

E-mail addresses: shiye@shanghaitech.edu.cn (Y. Shi), tuan.hoang@uts.edu.au (H.D. Tuan), a.savkin@unsw.edu.au (A.V. Savkin), Chin-Teng.Lin@uts.edu.au (C.-T. Lin), jianguo.zhu@sydney.edu.au (J.G. Zhu), poor@princeton.edu (H.V. Poor).

This work was supported in part by the Department of Science and Technology at Ho Chi Minh City, Vietnam under Grant 13/2018/HD-KHCNTT, in part by the Start-up research fund at Shanghaitech University, China, and in part by the Australian Research Council's Discovery Projects under Grant DP190102501, and in part by the U.S. National Science Foundation under Grants DMS-1736417 and ECCS-1824710.

Corresponding author.

Nomenclature				
Abbreviations				
ADMM	Alternating direction method of multipliers.			
DMPC	Distributed model predictive control.			
DR	Demand response.			
RES	Renewable energy resources.			
SDR	Semidefinite relaxation.			
AC-OPF	Alternating current optimal power flow.			
DC-OPF	Direct current optimal power flow.			
DR-OPF	Coordination between demand response and AC optimal power flow.			
Constants				
η	Weighting factor to trade-off the cost minimization and load fluctuation.			
$\overline{\theta}_{km}$	Voltage phase balance limitation of power line $(k, m) \in \mathcal{L}$.			
$\overline{P}_k^g(t)$	Upper bound of the active power generation of node $k \in \mathcal{G}$ at time slot t .			
$\overline{P}_k^r(t)$	Active RES generation of node $k \in C$ at time slot t .			
$\overline{Q}_k^g(t)$	Upper bound of the reactive power generation of node $k \in \mathcal{G}$ at time slot t .			
$\overline{Q}_k^r(t)$	Reactive RES generation of node $k \in C$ at time slot t .			
$\underline{P}_k^g(t)$	Lower bound of the active power generation of node $k \in \mathcal{G}$ at time slot t .			
$\underline{Q}_k^g(t)$	Lower bound of the reactive power generation of node $k \in \mathcal{G}$ at time slot t .			
h_{t}	Elastic supply capacity at time t.			
P_{avg}	Average power demand during the time			
408	period \mathcal{T} .			
r_k	Minimal power needed to complete the daily task of node $k \in \mathcal{N}$.			
S_{km}	Power capacity of line $(k, m) \in \mathcal{L}$.			
y_{km}	Admittance of line (k, m) .			
$\overline{\overline{V}}_k$	Upper bound of the amplitude of voltage injection at node $k \in \mathcal{N}$.			
\underline{V}_k	Lower bound of the amplitude of voltage injection at node $k \in \mathcal{N}$.			
$\overline{P}_k^c(t)$	Upper bound of the curtailable demand of node $k \in \mathcal{N}$ at time slot t , respectively.			
$\overline{P}_k^f(t)$	Upper bound of the flexible demand of node $k \in \mathcal{N}$ at time slot t , respectively.			
$P_k^l(t)$	Critical demand of node $k \in \mathcal{N}$ at time slot t .			
Sets				
\mathcal{C}	Set of nodes with RES.			

DR to improve energy efficiency and stabilize electricity price has been widely studied over the past few years. In [7], an incentive price mechanism was proposed for DR to ensure the users' truthfulness. A problem of residential energy consumption scheduling under price

\mathcal{G}	Set of nodes with generator.				
κ	Set of subsystems.				
\mathcal{L}	Set of power flow lines.				
\mathcal{N}	Set of nodes.				
\mathcal{T}	Set of time period.				
Variables					
$\mathbf{W}(t)$	Semidefinite matrix variable introduced to transfer the nonconvex power flow constraints with voltage product.				
$P_k^g(t)$	Active power generation by generator bus $k \in \mathcal{G}$ at time t .				
$P_k^r(t)$	RES curtailment of node $k \in C$ at time slot t .				
$Q_k^g(t)$	Reactive power generation by generator bus $k \in \mathcal{G}$ at time t .				
$V_k(t)$	Complex voltage variable of node $k \in \mathcal{N}$ at time t .				
$P_k^{\phi}(t)$	Auxiliary variable that collects the flexible demand, thermal demand and curtailable demand of node $k \in \mathcal{N}$ at time slot t , respectively.				
$P_k^c(t)$	The curtailable demand of node $k \in \mathcal{N}$ at time slot t .				
$P_k^d(t)$	Auxiliary variable that represents the total demand of node $k \in \mathcal{N}$ at time slot t .				
$P_k^f(t)$	The flexible demand of node $k \in \mathcal{N}$ at time slot t .				
$P_k^h(t)$	The thermal demand of node $k \in \mathcal{N}$ at time slot t .				

uncertainty and game interaction together with temporally-coupled DR constraints was studied in [8,9]. DR under spatially and temporally coupled constraints was addressed in [10] by a fast distributed algorithm, which is based on dual decomposition. In [11], a home energy management controller was proposed to minimize the daily curtailed energy in response to dynamic electricity pricing. This control problem is mathematically formulated by a mixed integer nonlinear optimization problem, which is then computed iteratively by an outer approximation algorithm. An incentive-based DR model for multiple energy carriers considering uncertainty of renewables and consumers was proposed in [12]. It should be emphasized that all the aforementioned works do not address the power grid operational constraints such as power balance, line capacity, and voltage and phasor bound in the DR, limiting the proliferation of DR in practical applications.

Recently, coordinations between DR and economic dispatch were initialized in [13], where the social welfare is maximized under the power balance constraints. Sharma et al. [14] investigated the coordination between DGs, battery energy storage systems and DR in a distribution network. This problem was formulated as a multi-objective optimization, which was solved by a genetic algorithm of centralized computation. A hierarchical control framework for the coordination between distributed energy resources and DR in a distribution network was proposed by Wu et al. [15]. A consensus-based distributed method was employed to handle the coordination problem. However, the important nodal voltage and its corresponding constraints were ignored in the model formulation of [15]. The authors in [16] examined DR in a time scheduling DC optimal power flow (DC-OPF) framework, which aims to minimize the total costs of generation and elastic power demand under the power grid operational and demand response constraints. An alternating direction method of multipliers (ADMM) approach in distributed computation is then employed to address this problem of convex optimization. The important issue of compensating the system error due to the DC approximation was not analyzed. In addition, DC-OPF is particularly unsuitable for distribution networks due to relatively low line X/R ratio [17,18]. Therefore, DR in an AC-OPF framework, which involves nonconvex but practical power flow constraints is more desirable compared to DR in the DC-OPF one in distribution networks. For simplification, coordination between DR and AC-OPF in this paper is abbreviated as DR-OPF.

As another important component in smart grid, RES should be taken into account for the DR-OPF. The output of RES is uncertain due to the random nature of meteorological factors [19]. To maintain a realtime balance between power demand and generation in smart grid, abundant renewable energy may have to be curtailed. Although conventional DGs can be scheduled to address the uncertainty issue when the RES is integrated to grid, it may not possible to provide sufficient support for high penetration of RES, which may trigger the likelihood of grid overvoltage conditions in smart grid [20]. RES curtailment by adjusting the real and reactive powers from renewable sources is thus needed to maintain the voltage stability. Therefore, RES curtailment should be considered in the DR-OPF coordination problem. As a recent work [20] showed, with the integration of high penetration of RES, the existing semidefinite relaxation (SDR) methods [21] for AC-OPF problem became inexact and thus lead to infeasible solution even for radial distribution networks.

DR-OPF coordination with RES curtailment can be driven either by centralized or distributed controllers. Central controller coordinates the whole system operation by using the full information access [22]. The system is prone to disruption once the centralized controller is in outage. Additionally, the computational and communication cost increases dramatically with the increase of system size since the centralized controller has to exchange the information with all the participants. Distributed controller of local controllers in each subsystem has attracted a serious attention [23,24]. Its first advantage is the reduction of computation power and communication bandwidth especially for large-scale systems. Moreover, it is capable of improving the system robustness and reliability even when contingency occurs. Importantly, unlike the centralized controller, which relies on gathering users' private data such as load profiles, the distributed controller can alleviate the potential concerns of privacy and security problems.

Nowadays, model predictive control (MPC) has emerged as a natural tool for online scheduling in power systems. A centralized MPC for power allocation in a plug-in electric vehicle with energy storage system was presented in [25]. A distributed MPC (DMPC) for energy systems was presented in [26], where a decomposition method was proposed to solve the large scale problem. In [27], a DMPC framework was developed to handle a combined environmental and economic dispatch problem. To the best of the authors' knowledge, there is no work on MPC for the joint coordination of DR-OPF with RES curtailment to not only minimize the total social costs consisting of power generation costs and RES curtailment costs and price-elastic demand costs but also manage the fluctuation of load demand under various demand response constraints and grid operational constraints. Its online implementation is very challenging because the future demand by appliances such as washing machines, dish washers, tumble dryers, electrical vehicles (EVs), etc. is unpredictable with unknown statistics, preventing the application of the conventional MPC [28]. Worse, the joint DR-OPF coordination with RES curtailment is inherently a difficult nonconvex optimization problem, which also raises computational intractability. Only very recently, a nonsmooth optimization algorithm was proposed in [29] for efficient computation of this type of nonconvex problems. To tackle the challenge in online computation for this problem, this paper proposes a novel DMPC, which does not require to predict future elastic power demand. Distributed computation is proposed to provide accurate coordination for the whole system and secure coordination with respect to users' privacy.

The main contribution of this paper is four-fold:

- This paper investigates online scheduling for joint coordination of demand response and AC-OPF problem, which considers various types of DR constraints, comprehensive power grid requirements and high penetration of RES curtailment. This problem is practical and attractive for smart grid although it is computationally intractable due to the nonconvex power flow constraints.
- In addition to minimization of the total operational costs, fluctuation of the overall load demand consisting of both baseline demand and price-elastic demand is flatted by regulating the total violation between real-time power demand and average power demand during the whole time horizon.
- The DR-OPF coordination is tackled in a distributed way, which can reduce computation and communication bandwidth especially for large-scale systems, improve system robustness and reliability, and alleviate the potential concerns of privacy and security issues.
- A novel ADMM-based DMPC algorithm is proposed for the online and distributed computation the DR-OPF coordination problem. It involves an iterative subroutine computation during the update procedure of primal variables that can efficiently handle the difficult nonconvex matrix rank-one constraint. A basic ADMM algorithm without this subroutine procedure may not even locate a feasible solution for this problem.

The rest of the paper is organized as follows. Section 2 is devoted to modeling of the multi-objective DR-OPF coordination with RES curtailment. Section 3 proposes a DMPC for its online implementation to maintain the network reliability and preserve users' privacy. A comprehensive simulation is conducted in Section 4 to confirm the viability of the proposed DMPC. Conclusions are drawn in Section 5.

Notation. j denotes the imaginary unit; $M \geq 0$ means that M is a Hermitian symmetric positive semi-definite matrix; $\operatorname{rank}(M)$ is the rank of the matrix M; $\Re(\cdot)$ and $\Im(\cdot)$ denote the real and imaginary parts of a complex quantity; $a \leq b$ for two complex numbers a and b is componentwise understood, i.e. $\Re(a) \leq \Re(b)$ and $\Im(a) \leq \Im(b)$; $\langle .,. \rangle$ is the dot product of matrices, while $\operatorname{diag}\{A_i\}$ denotes the matrix with diagonal blocks A_i and zero off-diagonal blocks; the cardinality of a set \mathcal{L} is denoted by $|\mathcal{L}|$.

2. System model and problem formulation

A smart grid that integrates a power grid, demand response, renewable energy resource and other interconnected smart grids, is shown in Fig. 1. This paper considers a distribution network with a set of buses $\mathcal{N} \triangleq \{1,2,\ldots,N\}$ connected through a set of lines $\mathcal{L} \subseteq \mathcal{N} \times \mathcal{N}$. Bus k is connected to bus m if and only if $(k,m) \in \mathcal{L}$. Denote by $\mathcal{N}(k)$ the set of other buses connected to bus k. $G \subseteq \mathcal{N}$ and $C \subseteq \mathcal{N}$ are the sets of those buses that are connected to DGs and RESs, respectively. Each bus is connected with active power demand E_k and reactive power demand Q_k^l .

2.1. Demand response

Electrical appliances can be generally classified into four categories: critical appliances, flexible appliances, thermal appliances and curtailable appliances. Critical appliances usually come from appliances such as refrigerators, electric cookers, etc. The power demand of critical appliances should be fixed without intervention during the specific time interval. Flexible appliances include the appliances whose power profiles can be controlled in response to electricity price variations whilst achieving their required energy usage during the period of operation. For example, EVs need to be charged to users' preferred status but the charging rate can be managed flexibly. Thermal appliances are those appliances that are used to maintain the indoor temperature within a

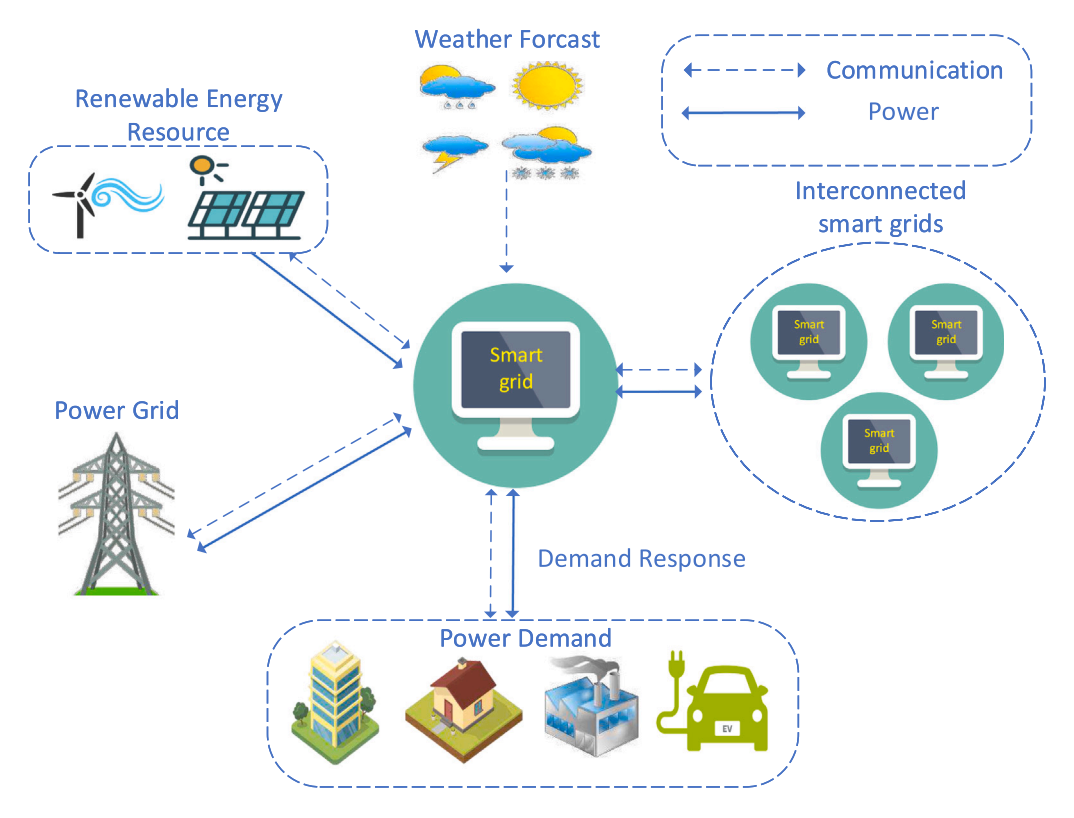


Fig. 1. The structure of a smart grid.

preferred range. Curtailable appliances include the appliance that can be turned off by operators to meet power demand requirements.

Different types of appliances will lead to different types of power demands in smart grid, i.e. critical demand, flexible demand, thermal demand and curtailable demand. Thus, we can divide the time period into T time slots $\mathcal{T} \triangleq \{1,2,\ldots,T\}$, and denote by $P_k^d(t)$, $P_k^l(t)$, $P_k^f(t)$, $P_k^h(t)$ and $P_k^c(t)$ the total demand, critical demand, flexible demand, thermal demand and curtailable demand of node k at time slot t, respectively.

The *critical demand* is independent of electricity price and can be predicted according to the historical data. In this paper, the critical demand $P_k^I(t)$ is assumed to be known beforehand.

The *flexible demand* is managed based on electricity price, providing that its accumulation must exceed a given threshold in order to complete the corresponding tasks each day. Accordingly, the flexible demand $P_k^f(t)$ is subject to the following constraints:

$$\sum_{t \in \mathcal{T}} P_k^f(t) \ge r_k, \quad k \in \mathcal{N}, \tag{1}$$

$$0 \le P_k^f(t) \le \overline{P}_k^f(t), \quad k \in \mathcal{N}, \ t \in \mathcal{T}, \tag{2}$$

where r_k is the minimum power needed to complete the daily task of node k and $\overline{P}_k^f(t)$ represents the upper bound of the flexible power demand of node k at time slot t.

The *thermal power demand* is consumed to preserve the indoor temperature within the user preferred settings. Following [11], the dwelling temperature T^{in} at each time slot t+1 at node k can be calculated by

$$T_k^{in}(t+1) = \epsilon_h T_k^{in}(t) + (1-\epsilon_h)(T_k^{out}(t) + \alpha P_k^h(t)), \quad k \in \mathcal{N}, \tag{3}$$

where $T^{in}(t)$ and $T^{out}(t)$ respectively represent the indoor and outdoor temperature, $\epsilon_h \in (0,1)$ is an inertia factor of the system and α is a parameter related to the thermal conductivity and the coefficient of performance. To maintain the indoor temperature within the user preferred interval, the following constraint is imposed:

$$T_l \le T_k^{in}(t) \le T_u, \quad k \in \mathcal{N}, \ t \in \mathcal{T},$$
 (4)

where T_l and T_u are respectively the lower and upper bound of preferred temperature. If $T^{out}(t) < T_l$, then α is a positive parameter; if $T^{out}(t) > T_u$, then α is a negative parameter; otherwise, α and $P_k^h(t)$ will be 0.

The *curtailable demand* represents the demand that is interruptible during the operation period. Denoting by $\overline{P}_k^c(t)$ the upper bound of the curtailable demand, $P_k^c(t)$ should be bounded by

$$0 \le P_{k}^{c}(t) \le \overline{P}_{k}^{c}(t), \quad k \in \mathcal{N}, \ t \in \mathcal{T}. \tag{5}$$

Suppose $P_k^d(t)$ is the total power demand of node k at time slot t. Obviously,

$$P_k^d(t) = P_k^l(t) + P_k^f(t) + P_k^h(t) + \overline{P}_k^c(t) - P_k^c(t), \quad k \in \mathcal{N}, \ t \in \mathcal{T}.$$
 (6)

It should be noted that $P_k^l(t)$ and $\overline{P}_k^c(t)$ are known values while $P_k^f(t)$, $P_k^h(t)$ and $P_k^c(t)$ are control variables.

2.2. Curtailment of renewable energy resource

With the increase of RES penetration in smart grid, the curtailment of RES has emerged as a natural way to maintain the balance between power demand and generation. Transmission limitation and generation flexibility are two main reasons for RES curtailment when high penetration of RES is integrated to grid. On the one hand, if the transmission capacity is limited, high penetration of RES will possibly result in a grid overvoltage condition. On the other hand, if the flexibility of generation output is constrained, the redundant renewable energy cannot be used locally and should be curtailed. Suppose the active and reactive powers of RES curtailment of node k at time slot t are $P_k^r(t)$ and $Q_k^r(t)$, respectively. At each time slot t, the following bound constraints should be imposed:

$$0 \le P_{\nu}^{r}(t) \le \overline{P}_{\nu}^{r}(t), \quad k \in \mathcal{C}, \tag{7}$$

$$-\overline{Q}_{k}^{r}(t) \le Q_{k}^{r}(t) \le \overline{Q}_{k}^{r}(t) \quad k \in \mathcal{C},$$
(8)

where $\overline{P}_k^r(t)$ and $\overline{Q}_k^r(t)$ are the known RES active and reactive power generation.

2.3. Power grid operation

At time slot t, let $V_k(t)$ be the complex voltage at bus k and let $P_k^g(t)+jQ_k^g(t)$ and $P_k^r(t)+jQ_k^r(t)$ respectively denote the complex power supplied by DGs and RES at bus k. Suppose that if a bus $k \in \mathcal{N} \setminus \mathcal{G}$, then $P_k^g(t)=Q_k^g(t)=0$. In addition, if a bus $k \in \mathcal{N} \setminus \mathcal{C}$, then $P_k^r(t)=Q_k^r(t)=0$.

$$V(t) = (V_1(t), \dots, V_N(t))^T \in \mathbb{C}^N$$
,

$$P^{g}(t) = (P_{1}^{g}(t), \dots, P_{N}^{g}(t))^{T} \in \mathbb{R}^{N},$$

$$Q^{g}(t) = (Q_{1}^{g}(t), \dots, Q_{N}^{g}(t))^{T} \in \mathbb{R}^{N},$$

Denote

$$Y = [Y_{km}]_{(k,m) \in \mathcal{N} \times \mathcal{N}} \in \mathbb{C}^{n \times n}$$

as the admittance matrix such that I=VY, where $I(t)=(I_1(t),\ldots,I_N(t))^T\in\mathbb{C}^N$ is the vector of current injection. For $t\in\mathcal{T}$, the following constraints associated with the active and reactive power generation $P_k^g(t)$ and $Q_k^g(t)$ and node voltage $V_k(t)$ must be fulfilled (see e.g. [21] and references therein):

$$P_{k}^{g}(t) \le P_{k}^{g}(t) \le \overline{P}_{k}^{g}(t), \quad k \in \mathcal{G}, \tag{9}$$

$$Q_{k}^{g}(t) \le Q_{k}^{g}(t) \le \overline{Q}_{k}^{g}(t), \quad k \in \mathcal{G},$$
(10)

$$V_k(t) \le |V_k(t)| \le \overline{V}_k(t), \quad k \in \mathcal{N},$$
 (11)

$$|V_k(t)V_m(t)^*y_{km}^*| \le S_{km}, \quad (k,m) \in \mathcal{L},$$
 (12)

$$|\arg(V_k)(t) - \arg(V_m)(t)| \le \overline{\theta}_{km}, \quad (k, m) \in \mathcal{L},$$
 (13)

where (9) and (10) are respectively the active and reactive power bounds of DGs with $\underline{P}_{g_k}(t)$, $\overline{P}_{g_k}(t)$ and $\underline{Q}_{g_k}(t)$, $\overline{Q}_{g_k}(t)$ denoted as the cor-

responding limitations; (11) represents the voltage magnitude bounds while $\underline{V}_k(t)$ and $\overline{V}_k(t)$ denote the corresponding lower and upper bounds, respectively; (12) is the constraint of line capacity limitation with $S_{km}(t)$ denoted as the upper limit of capacity for line (k,m); (13) guarantees the voltage balance in terms of the phase angle with $\overline{\theta}_{km}(t)$ denoted as the maximum voltage phase violation. Constraints (11)–(13) are indefinite quadratic inequality constraint, thus they are not convex.

2.4. Joint coordination of DR-OPF with RES curtailment

At any time slot t, the power supply and demand must be balanced for each bus k. Thus, the AC power flow equation involving power generated by DGs $P_k^g(t)+jQ_k^g(t)$, curtailed power of RES $P_k^c(t)+jQ_k^c(t)$, demand response $P_k^e(t)$ and nodal voltage $V_k(t)$ for all $t\in\mathcal{T}$ is formulated as:

$$E_k(t) = \sum_{m \in \mathcal{N}(k)} V_k(t) V_m(t)^* y_{km}^*, \quad k \in \mathcal{N}.$$
 (14)

where

$$E_{k}(t) = P_{k}^{g}(t) + \overline{P}_{k}^{r}(t) - P_{k}^{r}(t) - P_{k}^{d}(t) + j(Q_{k}^{g}(t) + \overline{Q}_{k}^{r}(t) - Q_{k}^{r}(t) - Q_{k}^{l}(t)).$$

$$(15)$$

(14) is an quadratic equality constraint, thus it is not convex.

For $\mathcal{V}=\{V(t)\}_{t\in\mathcal{T}}, \ \mathbf{P}^f=\{P_k^f(t)\}_{k\in\mathcal{N},t\in\mathcal{T}}, \ \mathbf{P}^h=\{P_k^h(t)\}_{k\in\mathcal{N},t\in\mathcal{T}}, \ \mathbf{P}^c=\{P_k^c(t)\}_{k\in\mathcal{N},t\in\mathcal{T}}, \ \mathbf{P}^\phi=\{\mathbf{P}^f,\mathbf{P}^h,\mathbf{P}^c\} \ \text{and} \ \mathbf{P}^r=\{P_k^r(t)\}_{k\in\mathcal{N},t\in\mathcal{T}}, \ \text{the} \ \text{first objective is to minimize the cost function constituting of power generation costs by the utilities, costs of curtailed power of RES and price-elastic demand costs by the customers, i.e.$

$$f(\mathcal{V}, \mathbf{P}^r, \mathbf{P}^{\phi}) = \sum_{t \in \mathcal{T}} (\sum_{k \in \mathcal{G}} f^g(P_k^g(t)) + \sum_{k \in \mathcal{K}} f^r(\overline{P}_k^r(t) - P_k^r(t)) + \sum_{k \in \mathcal{N}} \beta_t P_k^d(t)).$$

$$(16)$$

Here, $f^g(P_k^g(t))$ and $f^r(\overline{P}_k^r(t) - P_k^r(t))$ are respectively the cost function of real power generation by DGs and RES curtailment, which are linear

or quadratic in $P_k^g(t)$ and $P_k^r(t)$, respectively; and β_t is the known energy price related to demand response during the time slot t.

The second objective is to manage the power demand fluctuation by regulating the total violation between real time power demand and average power demand during the whole time horizon. The objective function of the multi-objective optimization is thus

$$\mathcal{F}(\mathcal{V}, \mathbf{P}^r, \mathbf{P}^\phi) = f(\mathcal{V}, P^r, P^\phi) + \eta \sum_{t \in \mathcal{T}} (\sum_{k \in \mathcal{N}} P_k^d(t) - P_{avg})^2,$$

where P_{avg} is the average power demand during the time period \mathcal{T} and is assumed to be known in advance, and η is a weighting factor to trade-off these two objectives. The average power demand P_{avg} is dependent on the total values of flexible demand, critical demand, thermal demand and curtailable demand. The total value of flexible demand is r_k as shown in (1), the critical demand is known beforehand, the thermal demand can be predicated according to a local weather forecast, the average curtailable demand is assumed to be $\frac{1}{2}\overline{P}_k^c$. Therefore, we can obtain an approximated average power demand. Thus, the task of the multi-objective DR-OPF coordination with RES curtailment is mathematically formulated by the following optimization problem:

$$\min \mathcal{F}(\mathcal{V}, \mathbf{P}^r, \mathbf{P}^\phi) \quad \text{s.t.} \quad (1) - (14), \ \forall t \in \mathcal{T}. \tag{17}$$

One can see that (12) in (17) is a nonconvex inequality constraint while (14) is nonconvex equality constraints, which pose a real computational challenge.

We now introduce the matrix variables

$$\mathbf{W}(t) = V(t)V(t)^H \in \mathbb{C}^{N \times N},\tag{18}$$

which must satisfy

$$\mathbf{W}(t) \ge 0,\tag{19}$$

$$rank(\mathbf{W}(t)) = 1 \tag{20}$$

to be qualified as the self-outer-product of vectors V(t) [29,30]. By replacing $W_{km}(t) = V_k(t)V_m(t)^*$ in (11)–(13) and (14), the optimization problem (17) for $\forall k \in \mathcal{N}, \ \forall t \in \mathcal{T}$ and $\forall (k,m) \in \mathcal{L}$ is reformulated as

$$\min \mathcal{F}(\mathcal{W}, \mathbf{P}^r, \mathbf{P}^{\phi})$$

$$E_k(t) = \sum_{m \in \mathcal{N}(k)} W_{km}(t) y_{km}^*,$$
 (21b)

$$(V_k(t))^2 \le W_{kk}(t) \le (\overline{V}_k(t))^2,$$
 (21c)

$$|W_{km}(t)y_{km}^*| \le \overline{S}_{km}(t), \tag{21d}$$

$$\mathfrak{F}(W_{km}(t)) \le \mathfrak{R}(W_{km}(t)) \tan \overline{\theta}_{km}(t),$$
 (21e)

$$\mathbf{W}(t) \succeq 0,\tag{21f}$$

$$rank(\mathbf{W}(t)) = 1, (21g)$$

where $W = \{\mathbf{W}(t)\}_{t \in \mathcal{T}}$; $\mathcal{F}(W, \mathbf{P}^r, \mathbf{P}^{\phi})$ is defined by substituting

$$V_k(t)V_m(t)^* = W_{km}(t), (k, m) \in \mathcal{L}$$

in the definition of $\mathcal{F}(\mathcal{V}, \mathbf{P}^r, \mathbf{P}^\phi)$; and (21c)–(21e) are respectively transformed from (11)–(13). More details can be referred to [29,30] and references therein. The problem difficulty is now concentrated on the matrix rank-one constraint (21g) as all other constraints in (21) are either linear or convex and thus computationally tractable. A recent work [20] showed that semi-definite relaxation (SDR) by dropping the rank-one constraint (21g) is inexact due to the penetration of RES, i.e. the SDR solution is not of rank-one and cannot be served even as a feasible point for the nonconvex problem (21). The simulation results of this paper also confirm this phenomenon.

Remark. Although DR-OPF coordination has been considered in some existing works, there is little work studying its online scheduling with

RES curtailment under the requirements of various types of DR constraints and comprehensive power grid operation constraints. In addition, the distributed computation for such a difficult nonconvex problem (21a) remains quite open. For instance, [31] studied a DR-OPF coordination problem with both elastic and inelastic demands in radial distribution networks and [32] investigated a DR-OPF coordination problem to improve voltage stability in transmission networks. However, neither [31] nor [32] considers the comprehensive demand response constraints and RES curtailment, limiting their applications in practice. The authors in [16] developed a distributed computation for DR-OPF coordination. Nevertheless, this method works only in a convex DC-OPF framework, which is not practical for distribution networks. To the best our knowledge, this paper is the first to develop distributed and online scheduling for DR-OPF coordination with RES curtailment under various DR and power grid constraints.

3. DMPC for DR-OPF coordination with RES curtailment

To address the online scheduling problem of DR-OPF coordination with RES curtailment, this section first provides a centralized MPC (CMPC) method and then proposes a consensus-based DMPC method based on the well-known ADMM method. The former will provide a baseline solution for the latter on this problem.

3.1. CMPC for the DR-OPF coordination with RES curtailment

Considering \mathbf{P}^f and $(\mathbf{P}^h, \mathbf{P}^c, \mathbf{P}^r, \mathcal{V})$ as the system state and control, Eqs. (2) provides state behavior with the end constraint (1) while the Eqs. (3)–(14) provide control constraints. The problem (17) is thus seen as a multi-objective control problem over the finite horizon [1, T]. However, the flexible power demand P^f such as EV's charging demand is unpredictably fluctuated in general, making the conventional MPC [28] inapplicable. As a matter of fact, the conventional MPC relies on two key steps at time t: predicting future events and minimizing a reference-based cost function by considering the plant over a short receding horizon [t', T]. Even though the flexible demand \mathbf{P}^f can be predicted by some possible methods, the prediction error is still unavoidable. We now follow the idea of [29,33] to address (17), which does not rely on any predictions of such information. We believe the new MPC method can even work under more uncertainties over the DGs as it does not require an exact prediction for future events.

At each time t', let $\varphi_k(t')$ be the minimal remaining demand for the elastic demand of node k, i.e. the cumulative elastic demand of node k during [t',T], which must satisfy the following constraints:

$$\sum_{t=t'}^{T} P_k^f(t) \ge \varphi_k(t'), \ k \in \mathcal{N}.$$
 (22)

Define

$$\begin{split} \mathcal{F}_{[t',T]} &= \sum_{t \in [t',T]} (\sum_{k \in \mathcal{G}} f^g(P_k^g(t)) + \sum_{k \in \mathcal{C}} f^r(\overline{P}_k^r(t) - P_k^r(t)) \\ &+ \sum_{k \in \mathcal{N}} \beta_t P_k^d(t) + \eta (\sum_{k \in \mathcal{N}} P_k^d(t) - P_{avg})^2). \end{split} \tag{23}$$

At each time t', we aim to solve the following optimization problem (24) over the prediction horizon [t',T] but only take the solution at current time slot t', i.e. $P^r(t')$, W(t') and $P^{\phi}(t')$ for online updating of problem (17),

$$\min \mathcal{F}_{[t',T]}$$
 s.t. (2)–(8), (21b)–(21g), (22). (24)

Note that (24) is still a very difficult optimization problem due to the nonconvex matrix rank-one constraint (21g). However, it is not necessary to assure (21g) satisfied for all $t \in [t'+1,T]$ since only the solution at time slot t' is used for online update in the MPC implementation. Thus, we consider the following simplified optimization problem (25) at time slot t' for saving the computation time:

$$\min \mathcal{F}_{[t',T]}$$
 s.t.

$$(21a)$$
- $(21f)$, (22) , $t \in [t', T]$, $(25a)$

$$rank(\mathbf{W}(t')) = 1. \tag{25b}$$

The optimization problem (25) is nonconvex due to the matrix rank-one constraint (25b), which can be computed by a nonsmooth optimization algorithm [30]. To make the paper self-contained, this algorithm is briefly recalled. Under the semidefinite condition (21f), it is clear $\operatorname{Trace}(\mathbf{W}(t')) - \bar{\lambda}(\mathbf{W}(t')) \geq 0$, where $\bar{\lambda}(\mathbf{W}(t'))$ is the maximal eigenvalue of the matrix $\mathbf{W}(t')$. Accordingly, the matrix rank-one constraint (25b) is equivalent to $\operatorname{Trace}(\mathbf{W}(t')) - \bar{\lambda}(\mathbf{W}(t')) = 0$. As such $\operatorname{Trace}(\mathbf{W}(t')) - \bar{\lambda}(\mathbf{W}(t'))$ can be used to measure the satisfaction of the matrix rank-one constraint $\operatorname{rank}(\mathbf{W}(t')) = 1$. We thus incorporate this term into the objective function to transform it into the following exactly penalized optimization problem with convex constraints:

$$\min F_{\mu} := F_{[t',T]} + \mu(\mathsf{Trace}(\mathbf{W}(t')) - \bar{\lambda}(\mathbf{W}(t'))) \quad \text{s.t. (39b)},$$
(26)

with a penalty parameter $\mu > 0$. The optimization (41) can be solved iteratively by the following convex problem:

min
$$F_{\mu}^{(\nu)} := F_{[t',T]} + \mu(\mathsf{Trace}(\mathbf{W}(t'))$$

 $-(\bar{w}^{(\nu)}(t'))^H \mathbf{W}(t')\bar{w}^{(\nu)}(t')$ s.t. (39b). (27)

where $\bar{w}^{(v)}(t')$ is the normalized eigenvector corresponding to the eigenvalue $\bar{\lambda}^{(v)}(t')$ at time slot t'. Note that

$$\bar{\lambda}(\mathbf{W}_{i}(t')) \ge (\bar{w}^{(\nu)}(t'))^{H} \mathbf{W}(t') \bar{w}^{(\nu)}(t'). \tag{28}$$

It is clear that we obtain $F_{\mu}^{(\nu)} \geq F_{\mu}$ and $F_{\mu}^{(\nu+1)} \leq F_{\mu}^{(\nu)}$. Therefore, $\mathbf{W}(t')^{(\nu+1)}$ is a better feasible point of (41) than $\mathbf{W}(t')^{(\nu)}$.

3.2. Consensus-based DMPC for DR-OPF coordination with RES curtailment

Consensus-based method is widely used for distributed computation in smart grid. A consensus algorithm is an interaction that specifies information exchange between each agent and its neighbors, and it will reach an agreement between these agents after convergence [34]. In this paper, we follow the consensus-based strategy to decompose the original problem (25) into several subproblems, each of which will be handled by an agent. Each agent solves the subproblem and then exchanges some information with its neighboring agents. The whole system will eventually reach a consensus solution between these agents.

In this paper, the whole system is first decomposed into K small interconnected subsystems, where a DMPC is formulated for each one. Fig. 2 presents the block diagram of the proposed DMPC for the interconnected subsystems, where each subsystem communicates with others based on a consensus strategy.

For $i \in \mathcal{K} = \{1, \dots, K\}$, define $\mathcal{R}_i = \{i_1, \dots, i_{R_i}\}$, which is the set of buses assigned to subsystem i. These bus sets must not be overlapped, i.e.

$$\mathcal{R}_i \cap \mathcal{R}_j = \emptyset, \ \forall i \neq j. \tag{29}$$

Let

$$\bar{\mathcal{R}}_i := \mathcal{R}_i \cup \{j | (j, i) \in \mathcal{L}, j \in \mathcal{R}_j, i \in \mathcal{R}_i, i \neq j\}$$
(30)

be an augmented subsystem to collect all the buses in \mathcal{R}_i and those buses in neighboring regions that are directly connected to the buses in \mathcal{R}_i . The vectors

$$\mathbf{V}_{i}(t) := (V_{i_{1}}(t), \dots, V_{i_{R_{i}}}(t))^{T}, \tag{31}$$

$$\mathbf{P}_{i}^{\phi}(t) := (P_{i_{1}}^{\phi}(t), \dots, P_{i_{\bar{R}_{i}}}^{\phi}(t))^{T}, \tag{32}$$

$$\mathbf{P}_{i}^{r}(t) := (P_{i_{1}}^{r}(t), \dots, P_{i_{\tilde{R}}}^{r}(t))^{T}. \tag{33}$$

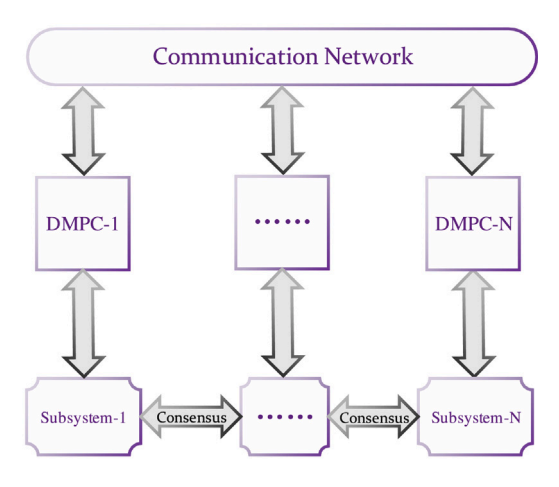


Fig. 2. The DMPC structure.

stack the complex voltages, elastic power demand, curtailed power of RES of buses in subsystem $\bar{\mathcal{R}}^i$. Let \mathcal{D}_{ii} be the set of buses shared by \bar{R}_i and \bar{R}_i . Per Fig. 3 for illustrative purpose, the original system is decomposed into three subsystems. Then $\mathcal{D}_{12} = \{1,5\}$, $\mathcal{D}_{13} = \{1,9\}$, and $D_{23} = \{5, 9\}$, which collect the duplicate nodes by $\bar{R}_1 \cap \bar{R}_2$, $\bar{R}_1 \cap \bar{R}_3$, and $\bar{R}_2 \cap \bar{R}_3$, respectively. Note that the information exchange of DMPC denoted by the arrows in Fig. 3 is quite light compared with that of the centralized algorithm. Furthermore, there is only limited information is shared between the regions to alleviate the potential privacy and security concerns. For the sake of simplicity, we assume that each augmented subsystem does not have overlapped nodes connected with RES, i.e. $C \cap D_{ij} = \emptyset$. To facilitate the proposed DMPC, the power network is decomposed by duplicating the voltage V(t) and demand $\mathbf{P}^{\phi}(t)$ at bus $k \in \mathcal{D}_{ii}$ of each subsystem. Accordingly, consensus constraints are added to make sure that the duplicated voltage in a subsystem is equal to the one in its neighboring subsystem. Define $\mathbf{W}_i(t) = \mathbf{V}_i(t)\mathbf{V}_i(t)^T$ and $\mathbf{W}_{ij}(t)$ as submatrix of $\mathbf{W}_i(t)$ collecting the rows and columns of $\mathbf{W}_{i}(t)$ corresponding to the indexes in \mathcal{D}_{ij} and define $\mathbf{P}_{ij}^{\phi}(t)$ as the subvector of $\mathbf{P}_{i}^{\phi}(t)$ collecting the entries of $\mathbf{P}_{i}^{\phi}(t)$ corresponding to the indexes in D_{ij} . Then, the consensus constraints are given by

$$\mathbf{W}_{ii}(t) = \mathbf{W}_{ii}(t), i, j \in \mathcal{K}, t \in [t', T]$$
 (34)

$$\mathbf{P}_{ii}^{\phi}(t) = \mathbf{P}_{ii}^{\phi}(t), \ i, j \in \mathcal{K}, \ t \in [t', T]. \tag{35}$$

For each subsystem $i \in \mathcal{K}$, define

$$\mathcal{F}^i_{[t',T]} = \sum_{t=t'}^T (\sum_{k \in \mathcal{G}_i} f(P^g_k(t)) + \sum_{k \in \mathcal{C}_i} f(P^r_k(t)) + \sum_{k \in \mathcal{N}_i} \beta_i P^\phi_k(t)).$$

At time t', we solve the following optimization problem (36) over the prediction horizon [t', T] but only take the solution at current time slot t', i.e. $\mathbf{W}_i(t')$, $\mathbf{P}_i^{\phi}(t')$ and $\mathbf{P}_i^{r}(t')$ for online update

$$\min_{\mathbf{W}_{i}, \mathbf{P}_{i}^{\phi}, \mathbf{P}_{i}^{c} \in \mathcal{B}_{i}, i \in \mathcal{K}} \sum_{i=1}^{K} \mathcal{F}_{[t',T]}^{i} \quad \text{s.t.}$$
(36a)

$$\mathbf{W}_{ii}(t') = \mathbf{W}_{ii}(t'), \ i, j \in \mathcal{K}, \tag{36b}$$

$$\mathbf{P}_{ii}^{\phi}(t') = \mathbf{P}_{ii}^{\phi}(t'), \ i, j \in \mathcal{K},\tag{36c}$$

$$\mathbf{W}_{i}(t) \succeq 0, \ i \in \mathcal{K}, \tag{36d}$$

$$rank(\mathbf{W}_i(t')) = 1, \ i \in \mathcal{K}, \tag{36e}$$

where \mathcal{B}_i is the convex domain corresponding to subsystem i such that the variables $\mathbf{W}_i(t)$, $\mathbf{P}_i^{\phi}(t)$ and $\mathbf{W}_i(t)$ satisfy the constraints (21a)–(21e)

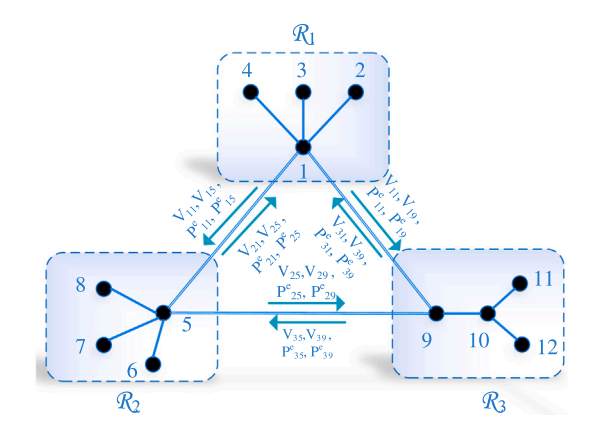


Fig. 3. Information exchange between subsystems.

with the respective replacement of the sets \mathcal{N} , \mathcal{G} , \mathcal{C} , and \mathcal{L} by the subsets \mathcal{N}_i , \mathcal{G}_i , \mathcal{C}_i , and \mathcal{L}_i , which are associated with the subsystem i. It is worth noting that, the consensus constraints (36b) and (36c) and the matrix rank-one constraints (36e) are only imposed at the current time slot t' during the MPC implementation. It is not worthy to assure them for the whole time horizon.

The DMPC problem (36) is seen nonconvex due to the multiple matrix rank-one constraints (36e). We now develop its distributed computations. Particularly, ADMM method [35–37] serves as the basis of the proposed distributed algorithm.

Let $\Gamma_{ij}(t) \in \mathbb{C}^{2\times 2}$ and $\gamma_{ij}(t) \in \mathbb{R}^{2\times 1}$ respectively denote the multipliers associated with constraint (36b) and constraint (36c). Let X collect $(\{\mathbf{W}_i(t)\}, \{\mathbf{P}_i^{\phi}(t)\}, \{\mathbf{P}_i^r(t)\}, \{\mathbf{W}_{ij}(t)\},$

 $\{F_{ij}(t)\}, \{\mathbf{P}_{ji}^{\phi}(t)\}, \{\gamma_{ij}(t)\}$). Consider the following partial augmented Lagrangian of (36)

$$\mathcal{L}(X) \triangleq \sum_{i=1}^{K} F_{[t',T]}^{i}(X) = \sum_{i=1}^{K} \mathcal{F}_{[t',T]}^{i} + \mathcal{F}_{AuL},$$
(37)

where

$$\mathcal{F}_{\text{AuL}} = \sum_{i=1}^{K} \sum_{t=t'}^{T} (\mathsf{Trace}(\Gamma_{ij}^{H}(t) \otimes (\mathbf{W}_{ij}(t) - \mathbf{W}_{ji}(t))))$$

$$+\gamma_{ij}^{H}(t)(\mathbf{P}_{ij}^{\phi}(t) - \mathbf{P}_{ji}^{\phi}(t)) + \frac{\delta}{2} \|\mathbf{W}_{ij}(t) - \mathbf{W}_{ji}(t)\|^{2} + \frac{\delta}{2} \|\mathbf{P}_{ii}^{\phi}(t) - \mathbf{P}_{ii}^{\phi}(t)\|^{2}), \tag{38}$$

where $\Gamma_{ij}^T(t) \otimes (\mathbf{W}_{ij}(t) - \mathbf{W}_{ji}(t)) = \Re(\Gamma_{ij}^H(t)\Re(\mathbf{W}_{ij}(t) - \mathbf{W}_{ji}(t))) + \Im(\Gamma_{ij}^H(t)\Im(\mathbf{W}_{ij}(t) - \mathbf{W}_{ji}(t)))$, $\delta > 0$ is a penalty parameter and $\|\cdot\|$ represents the Frobenius norm operator.

At each region $i \in \mathcal{K}$, we solve the following subproblem at time slot t',

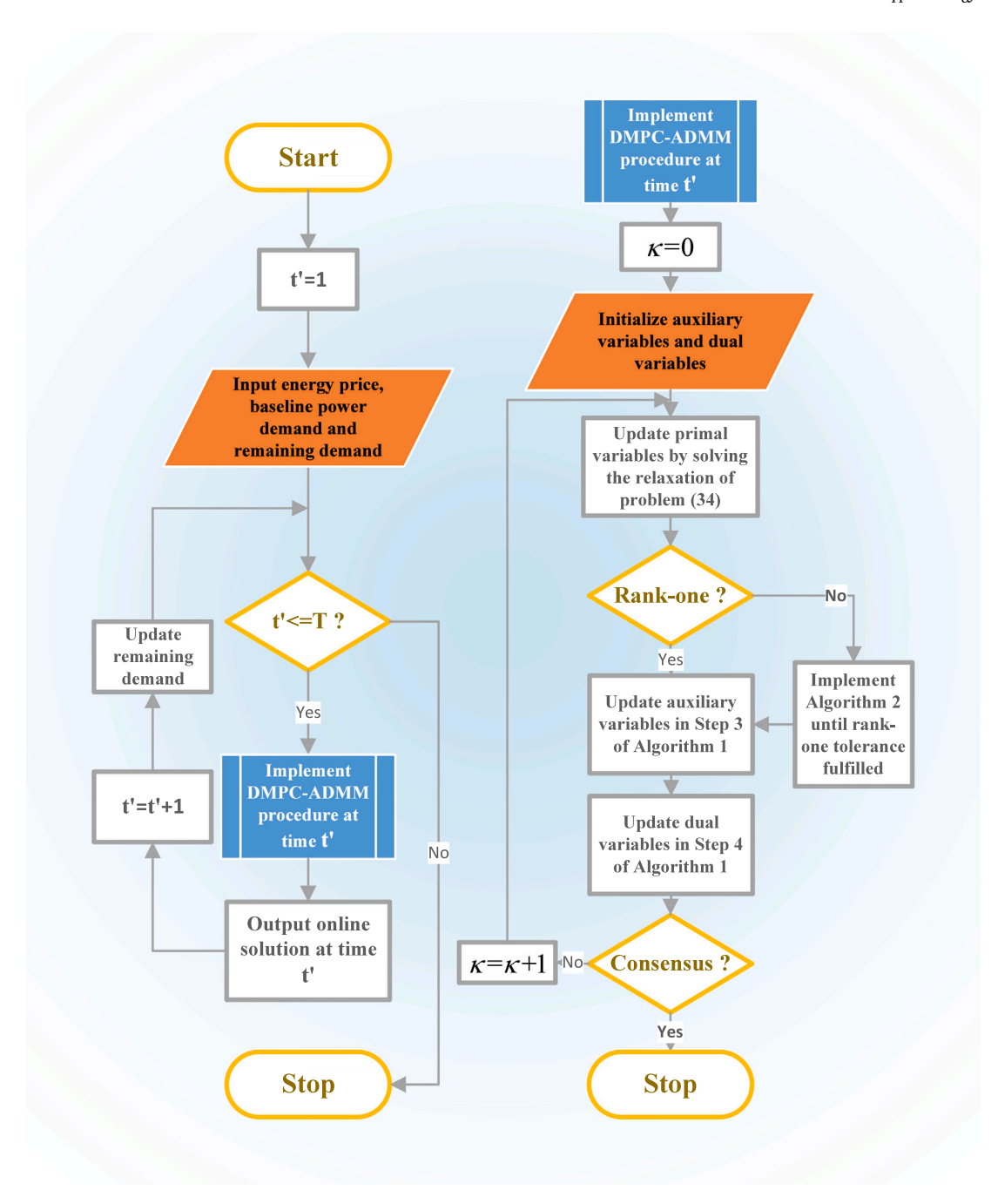
$$\min F_{[t',T]}^i(\boldsymbol{X}), \tag{39a}$$

s.t.
$$\mathbf{W}_{i}(t), \mathbf{P}_{i}^{\phi}(t), \mathbf{P}_{i}^{r}(t) \in \mathcal{B}_{i}, \ t \in [t', T]$$
 (39b)

$$rank(\mathbf{W}_i(t')) = 1. (39c)$$

Algorithm 1 is the pseudo-code for implementing the proposed ADMM. The sub-problem (39) in Step 2 of Algorithm 1 is nonconvex due to the matrix rank-one constraints (39c). Similar to the analysis in Section 3.1, we can transform (39) into the following exactly penalized optimization problem with convex constraints:

$$\min \ F_{\mu_i} := F_{[t',T]}^i(X) \\ + \mu_i(\mathsf{Trace}(\mathbf{W}_i(t')) - \bar{\lambda}_i(\mathbf{W}_i(t'))) \quad \text{s.t. (39b)}, \tag{41}$$



 $\textbf{Fig. 4.} \ \ \textbf{The flowchart of the proposed ADMM-based DMPC}.$

with a penalty parameter $\mu_i > 0$. The optimization (41) can be solved iteratively by the following convex problem:

min
$$F_{\mu_i}^{(v)} := F_{[t',T]}^i(X) + \mu_i(\text{Trace}(\mathbf{W}_i(t'))$$

 $-(\bar{w}_i^{(v)}(t'))^H \mathbf{W}_i(t')\bar{w}_i^{(v)}(t'))$ s.t. (39b). (42)

where $\bar{w}_i^{(v)}(t')$ is the normalized eigenvector corresponding to the eigenvalue $\bar{\lambda}_i^{(v)}(t')$ at time slot t'. Algorithm 2 provides the pseudo-code of the implementation to solve the sub-problem (39).

Fig. 4 illustrates the proposed DMPC. It is worth noting that we do not just apply a basic ADMM to solve the DMPC (36). Instead, we develop a new ADMM-based DMPC algorithm (Algorithm 1) for the distributed solution of this challenge DR-OPF coordination problem. Algorithm 1 involves an iterative subroutine computation (Algorithm 2) during the update procedure of primal variables in order to cope with

the difficult nonconvex matrix rank-one constraint (36e). Without this subroutine procedure, the ADMM-based DMPC algorithm (Algorithm 1) may not even locate a feasible solution for (36).

4. Simulation results

In this section, we discuss numerical simulations designed to test the proposed CMPC and DMPC algorithms, which could respectively provide a centralized and distributed solution for the joint DR-OPF coordination problem. Note that the former will provide a baseline solution for the latter on this problem. The optimality of the DMPC can be easily verified by checking the gap in objective values between the CMPC and DMPC. Since the DMPC algorithm is the main contribution of this paper, we will examine the optimal solutions obtained by the DMPC, including several types of demand response, nodal voltage and

Algorithm 1 ADMM-based DMPC (36)

- 1) Initialization: Set $\kappa = 0$ and initialize $\mathbf{W}_{ji}^{(\kappa)}(t)$, $(\mathbf{P}_{ji}^{\phi}(t))^{(\kappa)}$, $\Gamma_{ij}^{(\kappa)}(t)$ and $\gamma_{ii}^{(\kappa)}(t)$ for all $i \in \mathcal{K}$.
- 2) Update the primal variables: For each region i, input $\mathbf{W}_{ji}^{(\kappa)}(t)$, $(\mathbf{P}_{ji}^{\phi}(t))^{(\kappa)}$, $\Gamma_{ij}^{(\kappa)}(t)$ and $\gamma_{ij}^{(\kappa)}(t)$ and update $\mathbf{W}_{i}^{(\kappa+1)}(t)$, $(\mathbf{P}_{i}^{\phi}(t))^{(\kappa+1)}$ and $(\mathbf{P}_{i}^{r}(t))^{(\kappa+1)}$ concurrently by solving the sub-problem (39).
- 3) Update the auxiliary variables: Input $\mathbf{W}_i^{(\kappa+1)}(t)$, $(\mathbf{P}_i^{\phi}(t))^{(\kappa+1)}$ and $(\mathbf{P}_{ji}^r(t))^{(\kappa+1)}$ and update $\mathbf{W}_{ji}^{(\kappa+1)}(t)$ and $(\mathbf{P}_{ji}^{\phi}(t))^{(\kappa+1)}$ by solving the unconstrained problem:

$$\min \mathcal{F}_{AuL}$$
 (40)

4) Update the dual variables: For each region *i*, update $\Gamma_{il}^{(\kappa+1)}$ and $\gamma_{il}^{(\kappa+1)}$ by the following procedure,

$$\begin{split} & \Gamma_{ij}^{(\kappa+1)}(t') = \Gamma_{ij}^{(\kappa)}(t') + \delta(\mathbf{W}_{ij}^{(\kappa+1)}(t') - \mathbf{W}_{ji}^{(\kappa+1)}(t')), \\ & \gamma_{ii}^{(\kappa+1)}(t') = \gamma_{ii}^{(\kappa)}(t') + \delta((\mathbf{P}_{ij}^{\phi}(t'))^{(\kappa+1)} - (\mathbf{P}_{ii}^{\phi}(t'))^{(\kappa+1)}). \end{split}$$

5) Stopping criterion: If $||\mathbf{W}_{ij}^{(\kappa+1)}(t') - \mathbf{W}_{ji}^{(\kappa+1)}(t')|| \leq \epsilon$ and $||(\mathbf{P}_{ij}^{\phi}(t'))^{(\kappa+1)} - (\mathbf{P}_{ji}^{\phi}(t'))^{(\kappa+1)}|| \leq \epsilon$, stop the algorithm and output $\mathbf{W}_{i}^{(\kappa+1)}(t')$, $(\mathbf{P}_{i}^{\phi}(t'))^{(\kappa+1)}$ and $(\mathbf{P}_{i}^{c}(t'))^{(\kappa+1)}$ as the solution of (36); otherwise $\kappa = \kappa + 1$, go to step 2.

Algorithm 2 Subroutine computation for the sub-problem (39)

Initialization: Set v = 0, solve the problem (39) by dropping the rankone matrix constraints (39c) and output its solution $\mathbf{W}_i^{(v)}(t)$, $(\mathbf{P}_i^{\phi}(t))^{(v)}$ and $(\mathbf{P}_i^{r}(t))^{(v)}$.

if $\operatorname{rank}(\mathbf{W}_i^{(\nu)}(t')) = 1$ then terminate Algorithm 2 and accept $\mathbf{W}_i^{(\nu)}(t)$, $(\mathbf{P}_i^{\phi}(t))^{(\nu)}$ and $(\mathbf{P}_i^r(t))^{(\nu)}$ as the solution of (39);

elseSet v=v+1. Solve the optimization problem (42) to find its solution $\mathbf{W}_i^{(v+1)}(t)$ and $(\mathbf{P}_i^{\phi}(t))^{(v+1)}$, until $\mathsf{Trace}(W_i^{(v+1)}(t')) - (\bar{w}_i^{(v+1)}(t'))^H W_i^{(v+1)}(t') \bar{w}_i^{(v+1)}(t') \le \epsilon$ is satisfied for a given tolerance $\epsilon>0$ and output $\mathbf{W}_i^{(v+1)}(t)$, $(\mathbf{P}_i^{\phi}(t))^{(v+1)}$ and $(\mathbf{P}_i^r(t))^{(v+1)}$ as a found solution for (39).

end if

the fluctuation of power demand. Moreover, as the DMPC involves some penalized/weighting parameters, such as η and δ , we will also test the DMPC with different values of these parameters and analyze the corresponding results.

The simulation is tested on a simplified distribution network from the standard IEEE-123 test feeder. As shown in Fig. 5, there are three interconnected subsystems with 56 nodes, where 3 nodes are connected to DGs and 17 nodes are connected to RES. Its specific data of physical limits and cost function of the generation can be found in [38]. All simulations are implemented on a Core i7-8665 processor, while the convex optimization problems (41) and (42) are computed by the commercial solver Sedumi [39] interfaced by CVX [40]. The convergence criteria of ADMM procedure in the proposed algorithms is set as $\epsilon=10^{-3}$.

The time period is one day with one-hour time slot, i.e. T=24. The time-varying electricity price and baseline demand are plotted in Figs. 6 and 7. The data of time-varying electricity price and baseline demand used in this paper are based on the residential data of New South Wales (NSW) state, Australia on the 13th of November 2018 from [41]. The daily task required power demand $r_k, k \in \mathcal{N}$ is randomly generated as shown in Fig. 8, where nodes 7,21,33,56 have zero load demand according to the setting in [38]. The upper bound of flexible demand and curtailable demand of each node at each time slot are set to 100 kW and 50 kW, respectively. The thermal parameters are set as $\epsilon_h=0.8$

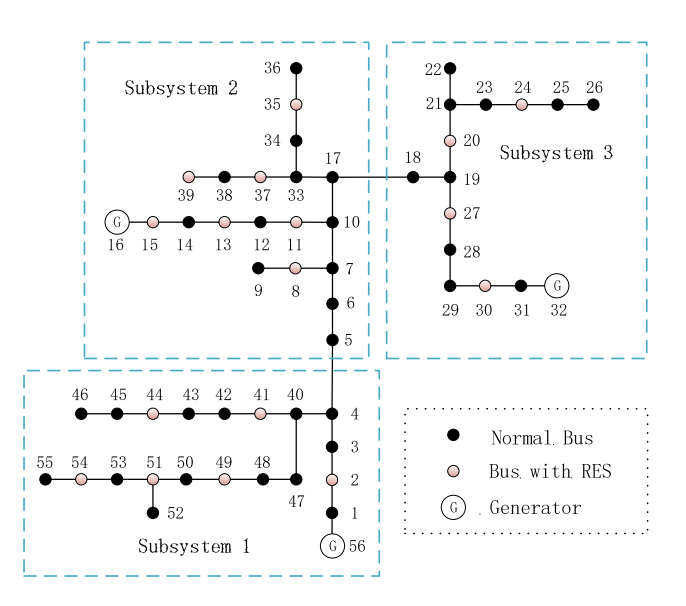


Fig. 5. Three subsystems in a simplified IEEE-123 test feeder.

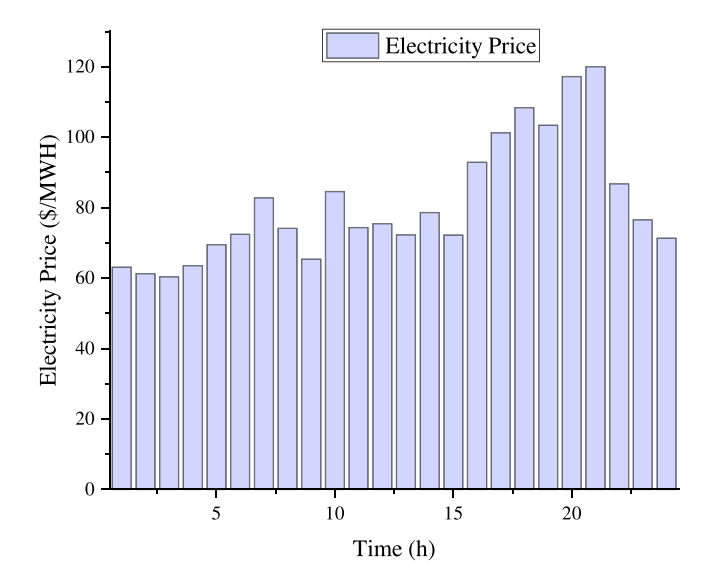


Fig. 6. Time-varying electricity pricing.

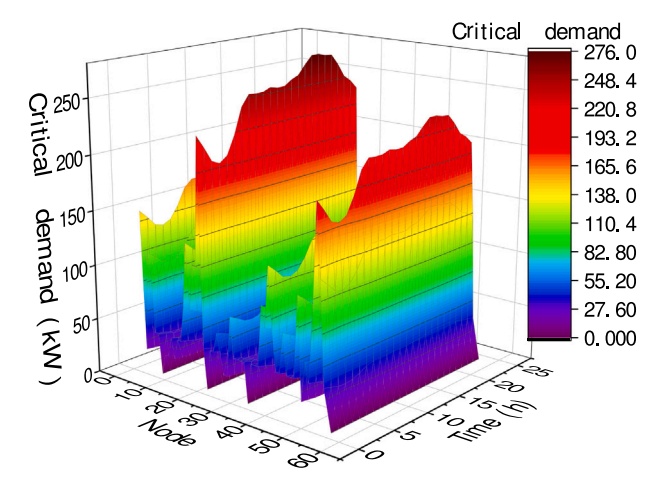


Fig. 7. Critical demand.

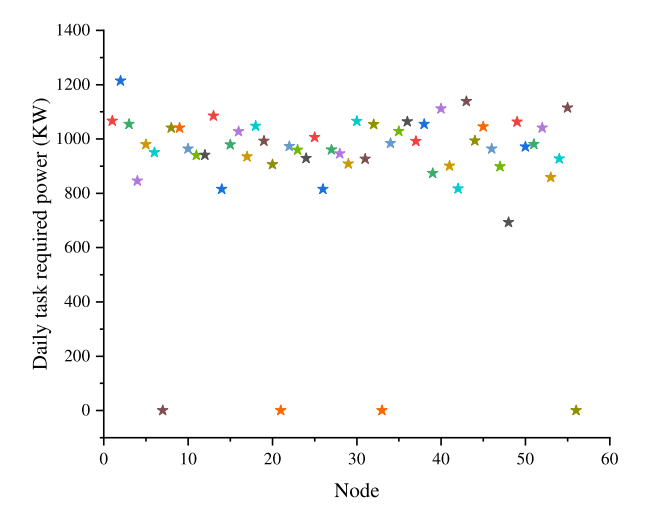


Fig. 8. The daily task required power demand r_k at each node.

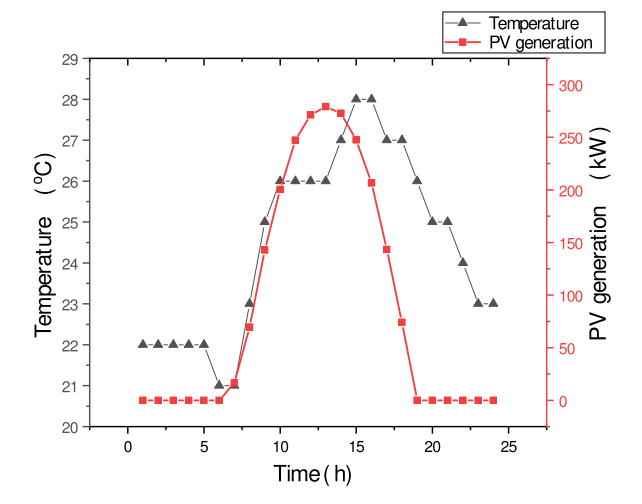


Fig. 9. Time-varying active PV generation $\overline{P}'(t)$ and outdoor temperature $T^{out}(t)$.

and $\alpha=\pm0.1$ °C/kW. The indoor temperature is preferred to maintain within [20 °C, 24 °C]. Photovoltaic (PV) power is used as the RES in this paper. The PV inverters are assumed to be located at the pink buses in Fig. 5. For each bus, the PV generation and real-time outdoor temperature are based on the real data from NSW on the 6th of January 2018 from [42] and [43]. Fig. 9 presents the time-varying active PV generation and outdoor temperature.

The simulation results are summarized in Table 1. Its first column contains various value of η . Obviously, the power load fluctuates less with larger η but at a higher total generation cost. The second column provides the corresponding value of the penalty parameter $\mu_i \equiv \mu$ in Algorithm 2. It is noted that the SDR for the subproblem (39) is inexact during time slot $t' \in \{11, 12, 13, 14, 15\}$ due to the high penetration of PV generation. Thus, Algorithm 2 must be implemented at these time slots in order to obtain the solution of (39). For all the tested cases at these time slots, Algorithm 2 converges within five iterations. The third column in Table 1 provides the total power generation costs of DGs, RES and price-elastic demand costs to customers using the CMPC for DR-OPF coordination problem (25). The average simulation time of online implementation of the CMPC at each time slot during the whole time period is given in the fourth column. The last two columns respectively provide the total costs and average simulation time obtained from the DMPC. Note that the total costs of the DMPC are lower bounded by the CMPC's. It can be seen that the difference

Table 1 Simulation results of CMPC and DMPC with various η and fixed $\delta = 100$.

η	μ	CMPC (\$)	Avg. T (s)	DMPC (\$)	Avg. T (s)
1	1	13 236.5	174.6	13 290.5	280.6
10	10	13833.7	145.8	13898.2	320.2
100	100	14065.9	182.5	14 125.5	335.4
1000	1000	14 457.8	167.4	14 540.3	317.4

between these two values in all these cases are within 1%, verifying the effectiveness of the proposed DMPC method. Although the DMPC costs more simulation time than the CMPC, its superiority concentrates on better privacy preservation and less communication bandwidth.

Fig. 10 presents the total power demand of the whole system with various values of η with fixed $\delta=100$. It can be seen in Fig. 10, the best performance of demand management is obtained by setting $\eta=1000$. However, a larger η leads to a higher total generation cost as Table 1 shows. Thus, we recommend to set $\eta=100$ to trade-off the generation cost and demand fluctuation. From Fig. 10 we can see that $\eta=100$ leads to much better performance of demand management than $\eta=1$ and $\eta=10$ does while it achieves only slightly worse power fluctuation compared to the result corresponding to $\eta=1000$. Therefore, we present the following simulation results based on the DMPC with $\eta=100$ and $\delta=100$ unless otherwise specified.

Figs. 11 and 12 show the flexible demand and voltage (unit p.u.) profile with $\eta = 100$. The obtained flexible demand intends to fill in the valley of Fig. 7, while the obtained value of voltage magnitude are bounded well within the range of [1.01,1.05]. In Fig. 13, we present the power generation P^g by DG, power generation \overline{P}^r by PV and power curtailment P^r of PV for subsystem 1 solved by implementing the DMPC method with $\eta = 100$ and $\delta = 100$. It can be seen that the obtained values of DG generation and PV curtailment are all well bounded. In addition, the DG generation remains low around noon time when the PV generation is quite high. Clearly, PV can be a very good supplement for DG. Fig. 14 shows the indoor temperature with and without control of the thermal appliances. We can see the indoor temperature increases with the outdoor one and reaches its peak value 26.4 °C at 19:00 pm without the control of thermal appliances. However, the indoor temperature with the control of thermal appliances is well bounded within the user preferred interval.

The convergence speed of the proposed DMPC method is investigated by using various value of ADMM parameter δ in the implementation. The convergence performance is shown in Fig. 15 by fixing $\eta=100$. It can be observed that large value of ADMM parameter δ does accelerate the convergence speed of the DMPC method. However, we still suggest to take proper value of ADMM parameter δ since larger δ lead to higher total costs.

5. Conclusion

This paper has considered an online scheduling for the joint DR-OPF coordination with high penetration of RES. Under comprehensive grid operational constraints, demand response constraints and RES curtailment constraints, not only the system overall operational cost is minimized but also the fluctuation of the overall power load is flattened. It should be noted that, with the integration of high penetration of RES, the SDR methods for AC-OPF problem becomes inaccurate even for radial distribution networks. Thus, the nonsmooth optimization Algorithm 2 should be employed to locate a feasible solution for this problem.

CMPC and DMPC have been developed in this paper respectively for the centralized and distributed computation of the online scheduling problem. The results for CMPC can serve as baselines for the DMPC's. Note that the DMPC is quite challenging as it requires distributed computation of a nonconvex optimization problem at each time slot. This paper has proposed a novel ADMM-based DMPC algorithm for its online

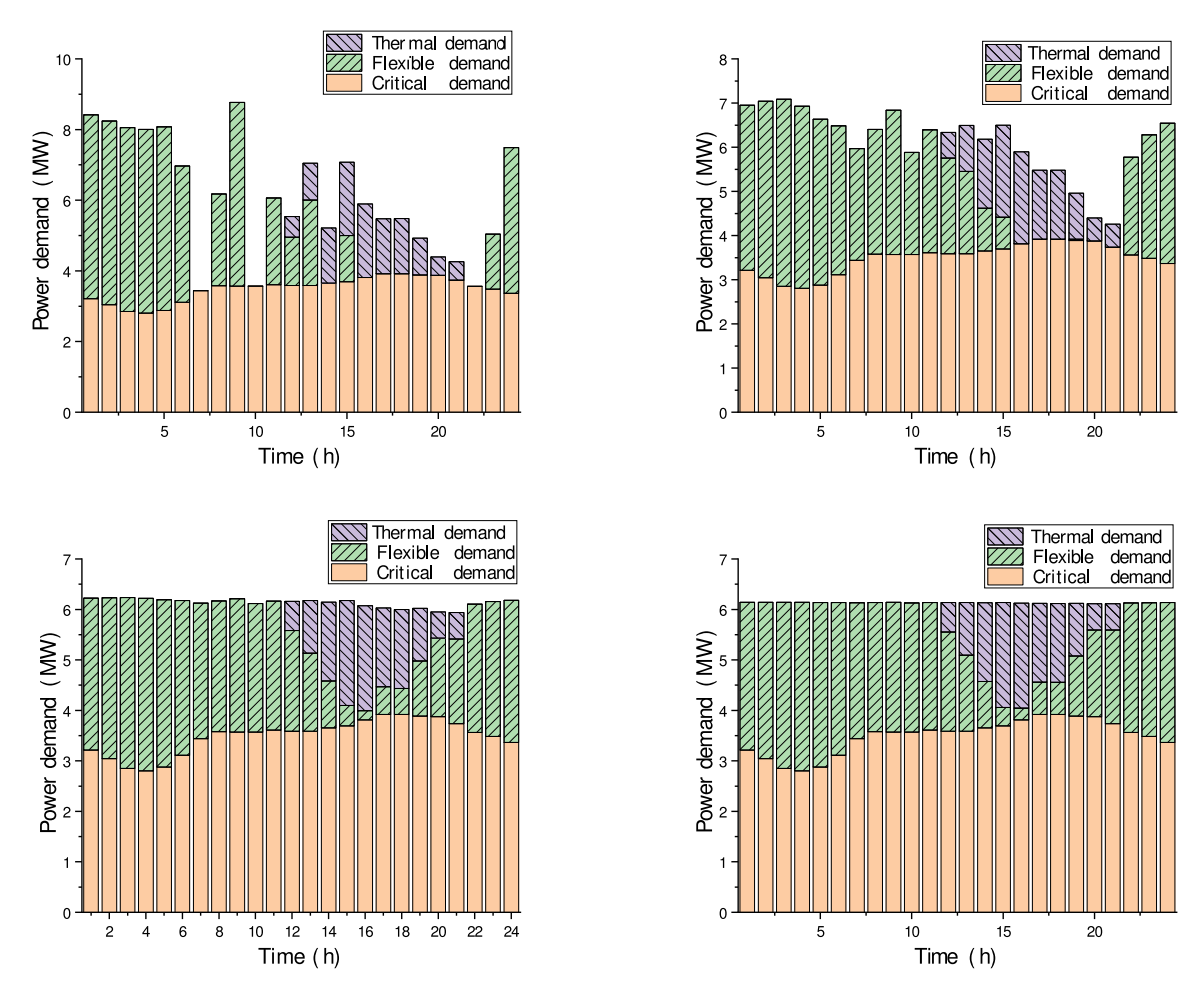


Fig. 10. Total demand with $\eta = 1, 10, 100, 1000$ from left-to-right then top-to-bottom.

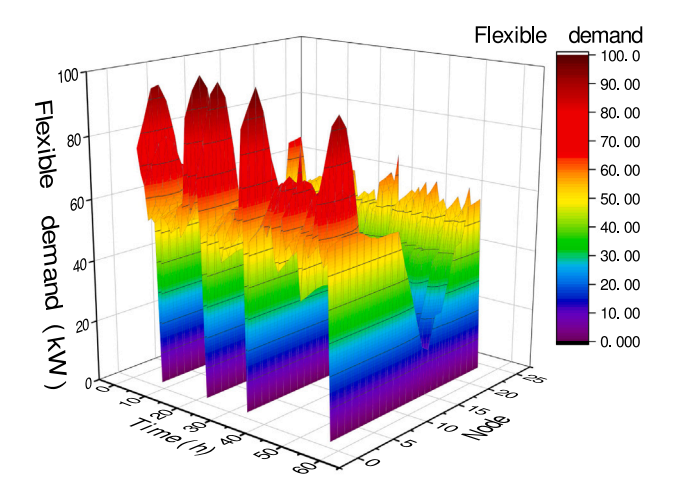


Fig. 11. Flexible demand with $\eta=100$ and $\delta=100$.

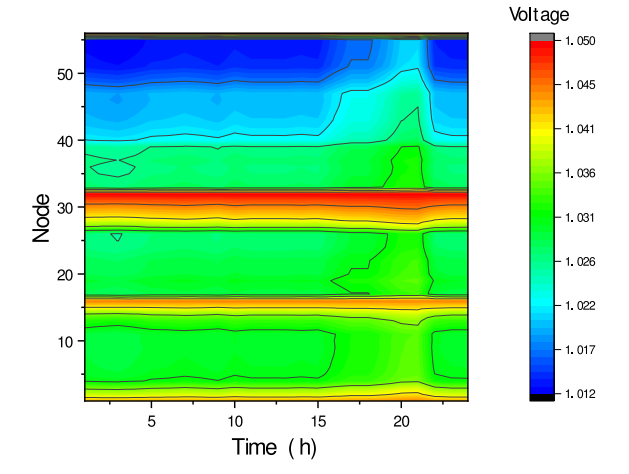


Fig. 12. Voltage (unit p.u.) profile with $\eta=100$ and $\delta=100$.

and distributed computation. It is worth noting that a basic ADMM cannot handle the DMPC problem due to the difficult nonconvex matrix rank-one constraint. The ADMM-based DMPC algorithm involves an iterative subroutine computation during the update procedure of primal variables to handle the difficult nonconvex matrix rank-one constraint. Without this subroutine procedure, the ADMM-based DMPC algorithm may not even locate a feasible solution. Moreover, the novel DMPC does not require to predict the future flexible power demand, increasing the

model practicability. The simulation results have shown that the objective values of the CMPC and DMPC are all within 1% of each other, further verifying the effectiveness of the proposed DMPC algorithm. The influence of some parameters on the model performance have also been investigated. It is quite intuitive to extend the developed ADMM-based DMPC method to various smart grid applications for distributed computation. An interesting topic for future work in this area is a

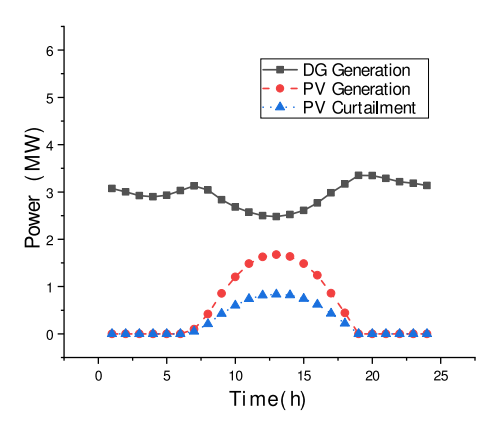


Fig. 13. Power generation by DG and PV and power curtailment of PV for subsystem 1 with n=100 and $\delta=100$.

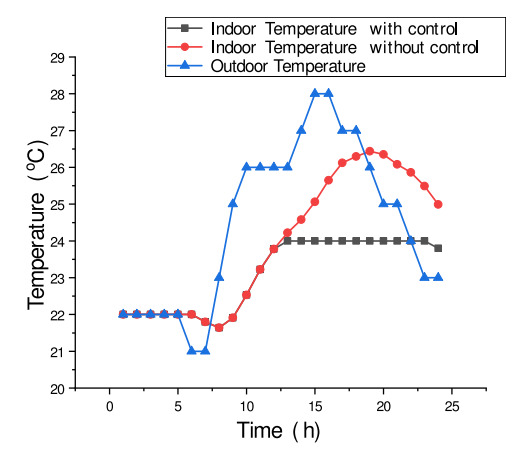


Fig. 14. Indoor temperature with and without control of the thermal demand.

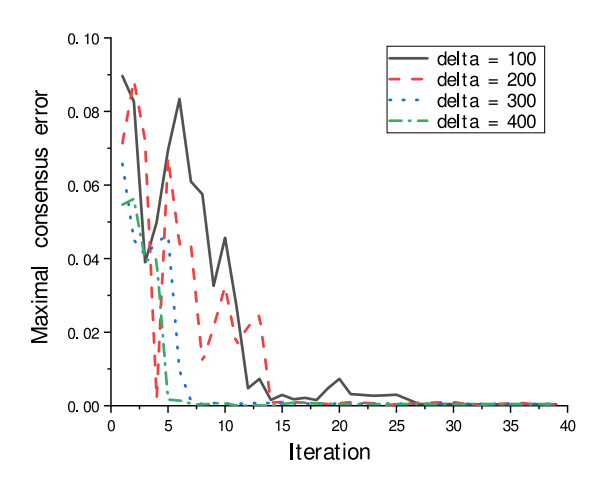


Fig. 15. The convergence performance under $\eta = 100$.

distributed online scheduling based on the DMPC method for electric vehicle charging/discharging in smart grid.

CRediT authorship contribution statement

Ye Shi: Conceptualization, Methodology, Software, Writing - original draft. Hoang Duong Tuan: Conceptualization, Methodology, Writing - review & editing, Supervision. Andrey V. Savkin: Funding acquisition, Writing - review & editing. Chin-Teng Lin: Writing - review &

editing. **Jian Guo Zhu:** Writing - review & editing. **H. Vincent Poor:** Writing - review & editing.

Declaration of competing interest

The authors declare that they have no known competing financial interests or personal relationships that could have appeared to influence the work reported in this paper.

Acknowledgments

We thank Dr. Ahmed S. Zamzam for kindly sharing the code of [20], which particularly points out that SDR does fail to locate a feasible solution for the AC OPF problem under high penetration of RES in radial distribution networks.

References

- Siano P. Demand response and smart grids a survey. Renew Sustain Energy Rev 2014;30:461–78.
- [2] Tuballa ML, Abundo ML. A review of the development of smart grid technologies. Renew Sustain Energy Rev 2016;59:710–25.
- [3] Ye M, Hu G. Game design and analysis for price-based demand response: An aggregate game approach. IEEE Trans Cybern 2017;47(3):720-30.
- [4] Wang X, Palazoglu A, El-Farra NH. Operational optimization and demand response of hybrid renewable energy systems. Appl Energy 2015;143:324–35.
- [5] Albadi MH, El-Saadany EF. A summary of demand response in electricity markets. Electr Power Syst Res 2008;78(11):1989–96.
- [6] Liu Z, Zhao Y, Wang X. Long-term economic planning of combined cooling heating and power systems considering energy storage and demand response. Appl Energy 2020;279:115819.
- [7] Ma J, Deng J, Song L, Han Z. Incentive mechanism for demand side management in smart grid using auction. IEEE Trans Smart Grid 2014;5(3):1379–88.
- [8] Deng R, Yang Z, Chen J, Asr NR, Chow M-Y. Residential energy consumption scheduling: A coupled-constraint game approach. IEEE Trans Smart Grid 2014;5(3):1340–50.
- [9] Deng R, Yang Z, Chen J, Chow M-Y. Load scheduling with price uncertainty and temporally-coupled constraints in smart grids. IEEE Trans Power Syst 2014;29(6):2823–34.
- [10] Deng R, Xiao G, Lu R, Chen J. Fast distributed demand response with spatially and temporally coupled constraints in smart grid. IEEE Trans Ind Inform 2015;11(6):1597–606.
- [11] Althaher S, Mancarella P, Mutale J. Automated demand response from home energy management system under dynamic pricing and power and comfort constraints. IEEE Trans Smart Grid 2015;6(4):1874-83.
- [12] Zheng S, Sun Y, Li B, Qi B, Zhang X, Li F. Incentive-based integrated demand response for multiple energy carriers under complex uncertainties and double coupling effects. Appl Energy 2021;283:116254.
- [13] Rahbari-Asr N, Ojha U, Zhang Z, Chow M-Y. Incremental welfare consensus algorithm for cooperative distributed generation/demand response in smart grid. IEEE Trans Smart Grid 2014;5(6):2836–45.
- [14] Sharma S, Niazi KR, Verma K, Rawat T. Coordination of different DGs, BESS and demand response for multi-objective optimization of distribution network with special reference to Indian power sector. Int J Electr Power Energy Syst 2020;121:106074.
- [15] Wu D, Lian J, Sun Y, Yang T, Hansen J. Hierarchical control framework for integrated coordination between distributed energy resources and demand response. Electr Power Syst Res 2017;150:45–54.
- [16] Wang Y, Wu L, Wang S. A fully-decentralized consensus-based ADMM approach for DC-OPF with demand response. IEEE Trans Smart Grid 2017;8(6):2637–47.
- [17] Tabatabaee S, Karshenas HR, Bakhshai A, Jain P. Investigation of droop characteristics and x/r ratio on small-signal stability of autonomous microgrid. In: Power electronics, drive systems and technologies conference (PEDSTC), 2011 2nd. 2011, p. 223–8.
- [18] Morstyn T, Hredzak B, Aguilera RP, Agelidis VG. Model predictive control for distributed microgrid battery energy storage systems. IEEE Trans Control Syst Technol 2018;26(3):1107–14.
- [19] Ellabban O, Abu-Rub H, Blaabjerg F. Renewable energy resources: Current status, future prospects and their enabling technology. Renew Sustain Energy Rev 2014;39:748–64.
- [20] Zamzam AS, Sidiropoulos ND, Dall'Anese E. Beyond relaxation and Newtonraphson: Solving AC OPF for multi-phase systems with renewables. IEEE Trans Smart Grid 2018:9(5):3966-75.
- [21] Lavaei J, Low SH. Zero duality gap in optimal power flow problem. IEEE Trans Power Syst 2012;27(1):92–107.

- [22] Olivares DE, Mehrizi-Sani A, Etemadi AH, Cañizares CA, Iravani R, Kazerani M, Hajimiragha AH, Gomis-Bellmunt O, Saeedifard M, Palma-Behnke R, et al. Trends in microgrid control. IEEE Trans Smart Grid 2014;5(4):1905–19.
- [23] Shamma JS. Cooperative control of distributed multi-agent systems. Wiley Online Library; 2007.
- [24] Zhao J, Dörfler F. Distributed control and optimization in DC microgrids. Automatica 2015;61:18–26.
- [25] Zhang S, Xiong R, Sun F. Model predictive control for power management in a plug-in hybrid electric vehicle with a hybrid energy storage system. Appl Energy 2017;185:1654–62.
- [26] Halvgaard R, Vandenberghe L, Poulsen NK, Madsen H, Jørgensen JB. Distributed model predictive control for smart energy systems. IEEE Trans Smart Grid 2016;7(3):1675–82.
- [27] Alejandro J, Arce A, Bordons C. Combined environmental and economic dispatch of smart grids using distributed model predictive control. Int J Electr Power Energy Syst 2014;54:65–76.
- [28] Camacho EF, Alba CB. Model predictive control. Springer Science & Business Media: 2013.
- [29] Shi Y, Tuan HD, Savkin AV, Duong TQ, Poor HV. Model predictive control for smart grids with multiple electric-vehicle charging stations. IEEE Trans Smart Grid 2019;10:2127–36.
- [30] Shi Y, Tuan HD, Tuy H, Su S. Global optimization for optimal power flow over transmission networks. J Global Optim 2017;69(3):745–60.
- [31] Khonji M, Chau C-K, Elbassioni K. Optimal power flow with inelastic demands for demand response in radial distribution networks. IEEE Trans Control Netw Syst 2016;5(1):513–24.

- [32] Yao M, Molzahn DK, Mathieu JL. An optimal power-flow approach to improve power system voltage stability using demand response. IEEE Trans Control Netw Syst 2019;6(3):1015–25.
- [33] Tuan HD, Savkin A, Nguyen TN, Nguyen HT. Decentralised model predictive control with stability constraints and its application in process control. J Process Control 2015;26:73–89.
- [34] Olfati-Saber R, Fax JA, Murray RM. Consensus and cooperation in networked multi-agent systems. Proc IEEE 2007;95(1):215–33.
- [35] Boyd S, Parikh N, Chu E, Peleato B, Eckstein J, et al. Distributed optimization and statistical learning via the alternating direction method of multipliers. Found Trends Mach Learn 2011;3(1):1–122.
- [36] Dall'Anese E, Zhu H, Giannakis GB. Distributed optimal power flow for smart microgrids.. IEEE Trans Smart Grid 2013;4(3):1464–75.
- [37] Magnússon S, Weeraddana PC, Fischione C. A distributed approach for the optimal power-flow problem based on ADMM and sequential convex approximations. IEEE Trans Control Netw Syst 2015;2(3):238–53.
- [38] Bolognani S. Approximate linear solution of power flow equations in power distribution networks, http://github.com/saveriob/approx-pf.
- [39] Sturm J. Using SeDuMi 1.02, a MATLAB toolbox for optimization over symmetric cones. Optim Methods Softw 1999;11–12:625–53.
- [40] Grant M, Boyd S. CVX: Matlab software for disciplined convex programming, version 2.1. 2014, http://cvxr.com/cvx.
- [41] Electricity. Australian NSW energy market operator. 2018, http://www.aemo. com.au/Electricity/National-Electricity-Market-NEM/Data-dashboard.
- [42] Photovoltaics. Australian NSW PV generation. 2018, http://pv-map.apvi.org.au/live.
- [43] Temperature. Australian NSW temperature. 2018, http://https://www.timeanddate.com/weather/australia/sydney/historic?month=1&year=2018.